

Schur-MI: Fast Mutual Information for Robotic Information Gathering

Kalvik Jakkala and Jason O’Kane and Srinivas Akella

Abstract—Mutual information (MI) is a principled and widely used objective for robotic information gathering (RIG), providing strong theoretical guarantees for sensor placement (SP) and informative path planning (IPP). However, its high computational cost—dominated by repeated log-determinant evaluations—has limited its use in real-time planning. This letter presents Schur-MI, a Gaussian process (GP) MI formulation that (i) leverages the iterative structure of RIG to *precompute* and reuse expensive intermediate quantities across planning steps, and (ii) uses a *Schur-complement* factorization to avoid large determinant computations. Together, these methods reduce the per-evaluation cost of MI from $\mathcal{O}(|\mathcal{V}|^3)$ to $\mathcal{O}(|\mathcal{A}|^3)$, where \mathcal{V} and \mathcal{A} denote the candidate and selected sensing locations, respectively. Experiments on real-world bathymetry datasets show that Schur-MI achieves up to a $12.7\times$ speedup over the standard MI formulation. Field trials with an autonomous surface vehicle performing adaptive IPP further validate its practicality. By making MI computation tractable for online planning, Schur-MI helps bridge the gap between information-theoretic objectives and real-time robotic exploration.

I. INTRODUCTION

The ability of autonomous robots to efficiently map and model unknown environments is a cornerstone of modern robotics. This field, known as robotic information gathering (RIG), underpins applications where human intervention is dangerous, inefficient, or impossible. Examples include monitoring the ocean floor and atmospheric phenomena, supporting search-and-rescue operations, and exploring planetary surfaces.

At the heart of RIG lie two fundamental challenges: sensor placement (SP) and informative path planning (IPP). The SP problem addresses the task of selecting a finite set of locations to deploy stationary sensors so as to maximize information about a spatial or spatiotemporal phenomenon. IPP generalizes this to a dynamic, sequential decision-making setting in which a mobile robot must choose a path—subject to constraints such as time or energy—to collect the most informative sequence of measurements.

A dominant paradigm for both SP and IPP is to model the unknown environment with a Gaussian process (GP), a non-parametric Bayesian model that provides both predictions and principled measures of uncertainty [1]. Within this framework, mutual information (MI) has emerged as an effective objective function [2], [3]. Unlike simpler uncertainty metrics such as variance or entropy, MI explicitly quantifies the reduction in uncertainty about the environment given a set of measurements, making it a principled and effective criterion for guiding exploration.

Over the past two decades, approaches for optimizing MI have evolved significantly. Seminal work showed that



Fig. 1: An autonomous surface vehicle mapping a lake during our field trials.

maximizing the submodular MI objective with a greedy algorithm over a discrete set of candidate locations yields *near-optimal* solutions [3]. To extend beyond discrete search, subsequent work has focused on continuous-space optimization using derivative-free, black-box methods such as genetic algorithms [4] and Bayesian optimization [5], [6], enabling direct optimization of complex path parameterizations.

Despite its strengths, MI remains underused in practice due to a fundamental *computational bottleneck*: each MI evaluation requires computing matrix determinants at a cost of $\mathcal{O}(m^3)$, where m is the number of candidate sensing locations in the environment. Because modern planners—from greedy selection to advanced adaptive frameworks—require numerous objective evaluations, this cubic cost often forces practitioners to abandon MI in favor of computationally cheaper but less informative proxies [7], [8]. Thus, the gap between MI’s theoretical appeal and its practical feasibility has persisted for decades.

This paper addresses this long-standing challenge by first identifying two key computational bottlenecks in the standard GP MI criterion. We then introduce precomputation to amortize terms that are independent of the selected sensing set, mitigating the first bottleneck. To address the second bottleneck, we propose an alternate RIG formulation that exposes additional reusable structure; however, this reformulation can both introduce a degeneracy and, in certain regimes, increase computational cost. We resolve these issues by deriving Schur-MI, which removes the degeneracy via a perturbed surrogate candidate set and substantially reduces computation cost by leveraging a Schur-complement fac-

torization with precomputation, making MI-based planning feasible for real-time, adaptive, and large-scale RIG.

II. RELATED WORK

Our work, which aims to accelerate the computation of mutual information (MI), is framed within three key areas of research: the formulation of information-theoretic objectives, the design of planners that optimize them, and the need for scalable computation.

A. Information-Theoretic Objectives for RIG

The effectiveness of an informative path is determined by the objective function it seeks to optimize. While early approaches relied on simple geometric criteria like coverage [9], [10], modern methods leverage probabilistic models of the environment to guide planning [3]. Gaussian Processes (GPs) [1] have become the predominant model, giving rise to several information-theoretic metrics.

A common and computationally simple metric is the predictive variance (or entropy) at unsensed locations. The strategy of greedily sampling points of highest variance is intuitive but can lead to suboptimal placements, often clustering sensors along the boundaries of the search space [3]. Other classical criteria from the field of optimal experimental design, such as A-, D-, and B-optimality [7], have also been adapted but suffer from similar limitations.

The MI criterion, proposed by Caselton and Zidek [2], stands out as a more robust metric. By quantifying the reduction in uncertainty over all *unobserved* locations, MI naturally encourages placements that are centrally located and highly informative.

Krause et al. [3] demonstrated that while maximizing MI is NP-complete, its submodularity allows a greedy algorithm to achieve a *near-optimal solution with a $(1 - 1/e)$ approximation guarantee*. Furthermore they proposed an efficient approximation that sparsifies the covariance matrix to reduce inversion costs, thereby lowering the overall computational complexity from $\mathcal{O}(sm^4)$ to $\mathcal{O}(sm)$, where s and m denote the numbers of sensing and candidate locations, respectively. However, this sparsification approach sacrifices critical long-range correlations captured by non-stationary kernels, thus limiting its applicability to stationary settings.

B. Optimization and Planning Algorithms

Given an information objective, a planner's role is to find a path that optimizes the objective. Key methods are summarized below:

Discrete-Space Greedy Optimization: The foundational method, enabled by MI's submodularity, is a greedy algorithm that iteratively adds the most informative location from a discrete set of candidates. This approach is simple and guaranteed to be near-optimal, but it is also myopic and limited to predefined candidate locations [3], [11].

Continuous-Space Optimization: To plan paths in continuous spaces, researchers have employed derivative-free, black-box optimization techniques like genetic algorithms [4] and Bayesian optimization [5], [6]. These methods can handle

complex path parameterizations but treat the MI objective as a black box, requiring numerous expensive evaluations that worsen the computational bottleneck.

Adaptive Planning: More advanced planners address the adaptive nature of IPP, where decisions are made online as new data is collected [12], [7]. These methods often frame the problem as a partially observable Markov decision process (POMDP) and use techniques like Monte Carlo tree search (MCTS). Notably, these planners often abandon the MI objective for computationally cheaper proxies like variance reduction to maintain tractability.

Learning-Based Approaches: A recent trend involves using machine learning, particularly Reinforcement Learning (RL) and Imitation Learning (IL), to learn complex, reactive planning policies [13], [14]. While powerful, these methods do not eliminate the underlying issue; if the policy is trained using an MI-based reward signal, the training process itself will require a massive number of expensive MI calculations.

C. Scalability and Efficiency in RIG

The computational burden of GP-based planning with the MI objective is a major theme in literature. As robotic applications grow in scale and complexity, so does the need for efficient methods. Research has addressed this problem from the following angles:

Approximating the Objective: One common strategy is to replace or approximate the MI objective [15], [16]. Some methods use simpler proxies like variance reduction or develop lower-dimensional projections to create a bound on MI. Others create differentiable approximations of MI to enable faster, gradient-based optimization [7], [8]. Notably, Ott et al. [12] proposed approximating MI by replacing determinant operations with trace operations.

Improving the Model: Another approach focuses on the underlying GP model itself [17], [18], [19]. This includes using more efficient model variants like Sparse or Variational Gaussian Processes to handle large datasets or developing non-stationary kernels for more accurate uncertainty estimates. These methods improve the model from which MI is computed but do not accelerate the MI calculation itself.

Our work addresses a critical gap left by these complementary efforts. While planners have grown more powerful and models more expressive, the MI objective has remained computationally prohibitive. Instead of relying on approximations, we tackle this bottleneck directly. Leveraging the Schur complement and precomputation-based factorization, we accelerate MI computation, enabling advanced, large-scale, and adaptive planning frameworks to fully realize the potential of state-of-the-art robotic information gathering.

III. PRELIMINARIES: GAUSSIAN PROCESSES

To formally model a phenomenon and quantify information, we use Gaussian processes (GPs) [1], a powerful non-parametric tool from Bayesian statistics for modeling correlated data.

A Gaussian Process is a collection of random variables, any finite number of which have a joint Gaussian distribution.

It is important to note that despite their name, GPs are not limited to modeling phenomena that are themselves Gaussian distributed. Rather, a GP defines a distribution over functions, making it a flexible tool for a wide range of regression problems.

The method places a GP prior over an unknown function:

$$f(\mathbf{x}) \sim \mathcal{GP}(m(\mathbf{x}), k(\mathbf{x}, \mathbf{x}')). \quad (1)$$

This process is completely specified by a mean function $m(\mathbf{x})$ and a covariance function (or kernel) $k(\mathbf{x}, \mathbf{x}')$. The mean function, often assumed to be zero after data normalization, represents the expected value of the function at location \mathbf{x} . The kernel function defines the covariance between the function values at two locations, \mathbf{x} and \mathbf{x}' :

$$k(\mathbf{x}, \mathbf{x}') = \text{cov}(f(\mathbf{x}), f(\mathbf{x}')). \quad (2)$$

The kernel encodes our prior beliefs about the properties of the function, such as its smoothness and length-scale. A common choice is the squared exponential (or radial basis function (RBF) kernel):

$$k(\mathbf{x}, \mathbf{x}') = \sigma_f^2 \exp\left(-\frac{\|\mathbf{x} - \mathbf{x}'\|^2}{2l^2}\right), \quad (3)$$

where the signal variance σ_f^2 controls the overall variance of the function, and the length-scale l determines how quickly the correlation between points decays with distance.

Given a set of n noisy observations $\mathcal{D} = \{\mathbf{X}, \mathbf{y}\} = \{(\mathbf{x}_i, y_i), i = 1, \dots, n\}$, where $y_i = f(\mathbf{x}_i) + \epsilon_i$ and the noise ϵ_i is assumed to be i.i.d. Gaussian with variance σ_n^2 , we can compute the posterior predictive distribution for a new test point \mathbf{x}_* . This posterior is also a Gaussian process, $p(f_* | \mathbf{X}, \mathbf{y}, \mathbf{x}_*) = \mathcal{GP}(\mu_*, \sigma_*^2)$, with mean μ_* and variance σ_*^2 given by:

$$\begin{aligned} \mu_* &= \mathbf{K}_{*n}(\mathbf{K}_{nn} + \sigma_n^2 \mathbf{I})^{-1} \mathbf{y}, \\ \sigma_*^2 &= \mathbf{K}_{**} - \mathbf{K}_{*n}(\mathbf{K}_{nn} + \sigma_n^2 \mathbf{I})^{-1} \mathbf{K}_{n*}, \end{aligned} \quad (4)$$

where $\mathbf{K} = k(\cdot, \cdot)$ are the covariance matrices. The covariance matrix subscripts indicate the variables used to compute it: $*$ for the test input \mathbf{x}_* and n for the training inputs \mathbf{X} .

IV. PROBLEM STATEMENT

Robotic information gathering (RIG) concerns the problem of selecting informative sampling locations to efficiently estimate an unknown spatial or spatiotemporal field $\mathcal{X} \subset \mathbb{R}^d$. For the purposes of estimation and decision-making, the environment is discretized into a set of m evaluation points, $\mathcal{V} = \{x_1, \dots, x_m\} \subset \mathcal{X}$. The goal is to infer an underlying field $y : \mathcal{V} \rightarrow \mathbb{R}^p$, representing environmental quantities such as ocean temperature, salinity, or terrain elevation.

We aim to select a subset of s sampling locations $\mathcal{A} = \{x_i \in \mathcal{V} \mid i = 1, \dots, s\}$, with $s \ll m$, at which noisy measurements are obtained as $y_i = y(x_i) + \epsilon_i$, where $\epsilon_i \sim \mathcal{N}(0, \Sigma_\epsilon)$ models sensor noise. The objective is to choose \mathcal{A} such that the collected data maximizes the expected

information about $y(\cdot)$ over \mathcal{V} according to an information metric $\mathbb{I}(\cdot)$.

This work focuses on *mutual information (MI)* as the optimization criterion, owing to its strong theoretical foundations and near-optimal approximation guarantee. The MI-based RIG problem is typically formulated as selecting a subset of sensing locations \mathcal{A} that maximizes the MI between the sampled and unsampled regions:

$$\mathcal{A}^* = \arg \max_{\mathcal{A} \subset \mathcal{V}} \mathbb{I}(\mathcal{A}; \mathcal{V} \setminus \mathcal{A}), \quad (5)$$

where \mathcal{V} denotes the complete set of candidate sensing locations. The MI between two sets of random variables is defined as follows, with $H(\cdot)$ denoting entropy [20]:

$$\begin{aligned} \mathbb{I}(\mathcal{A}; \mathcal{V} \setminus \mathcal{A}) &= H(\mathcal{A}) - H(\mathcal{A} \mid \mathcal{V} \setminus \mathcal{A}) \\ &= H(\mathcal{A}) + H(\mathcal{V} \setminus \mathcal{A}) - H(\mathcal{V}). \end{aligned} \quad (6)$$

We model the underlying phenomenon using Gaussian Processes (GPs), which enable closed-form computation of entropy and MI through their covariance structure. The central problem is to compute MI for a given set \mathcal{A} of sampling locations selected from the candidate locations \mathcal{V} . However, evaluating MI under GPs is computationally demanding, requiring $\mathcal{O}(m^3)$ operations for matrix inversions and determinant evaluations. This computational burden significantly limits the scalability of MI-based methods for real-time and large-scale planning.

To address this challenge, we propose an efficient formulation of MI for RIG that preserves the theoretical rigor of the original information-theoretic objective while substantially reducing computational complexity. This enables principled, MI-driven decision-making in real-world, time-critical robotic exploration and sensing applications.

V. METHOD

Our goal is to select sensing locations that maximize mutual information (MI) under a Gaussian process (GP) model, while keeping the computation fast enough for real-time robotic information gathering (RIG). We first introduce the standard GP MI criterion and identify its dominant computation cost bottlenecks. Next, we show how simple precomputation amortizes repeated costs and motivates an alternate RIG objective that exposes additional reusable structure. Finally, we derive an equivalent Schur-complement MI formulation which, combined with precomputation and a nondegenerate surrogate candidate set, yields an efficient objective suitable for real-time RIG.

A. Standard Mutual Information Criterion

Under a GP prior, the entropy of the latent variables [20] evaluated at a set of inputs \mathcal{A} with covariance $\mathbf{K}_{\mathcal{A}, \mathcal{A}}$ is

$$H(\mathcal{A}) = \frac{s}{2} \ln(2\pi e) + \frac{1}{2} \ln \det(\mathbf{K}_{\mathcal{A}, \mathcal{A}}), \quad (7)$$

where $s = |\mathcal{A}|$ and $\det(\cdot)$ denotes the matrix determinant. For clarity of exposition, we omit the observation noise variance σ_n^2 (equivalently, one may replace \mathbf{K} by $\mathbf{K} + \sigma_n^2 \mathbf{I}$).

Substituting this entropy into the set-based MI definition (Equation (6)) gives

$$\begin{aligned}
\mathbb{I}(\mathcal{A}; \mathcal{V} \setminus \mathcal{A}) &= H(\mathcal{A}) + H(\mathcal{V} \setminus \mathcal{A}) - H(\mathcal{V}) \\
&= \frac{s}{2} \ln(2\pi e) + \frac{1}{2} \ln \det(\mathbf{K}_{\mathcal{A}\mathcal{A}}) \\
&\quad + \frac{r}{2} \ln(2\pi e) + \frac{1}{2} \ln \det(\mathbf{K}_{(\mathcal{V} \setminus \mathcal{A})(\mathcal{V} \setminus \mathcal{A})}) \\
&\quad - \frac{m}{2} \ln(2\pi e) - \frac{1}{2} \ln \det(\mathbf{K}_{\mathcal{V}\mathcal{V}}) \\
&= \frac{1}{2} \ln \det(\mathbf{K}_{\mathcal{A}\mathcal{A}}) + \frac{1}{2} \ln \det(\mathbf{K}_{(\mathcal{V} \setminus \mathcal{A})(\mathcal{V} \setminus \mathcal{A})}) \\
&\quad - \frac{1}{2} \ln \det(\mathbf{K}_{\mathcal{V}\mathcal{V}}) \\
&= \frac{1}{2} \ln \left[\frac{\det(\mathbf{K}_{\mathcal{A}\mathcal{A}}) \cdot \det(\mathbf{K}_{(\mathcal{V} \setminus \mathcal{A})(\mathcal{V} \setminus \mathcal{A})})}{\det(\mathbf{K}_{\mathcal{V}\mathcal{V}})} \right].
\end{aligned} \tag{8}$$

Here, $m = |\mathcal{V}|$ and $r = |\mathcal{V} \setminus \mathcal{A}| = m - s$. Evaluating Equation (8) is dominated by computing $\det(\mathbf{K}_{\mathcal{V}\mathcal{V}})$ at cost $\mathcal{O}(m^3)$, followed by $\det(\mathbf{K}_{(\mathcal{V} \setminus \mathcal{A})(\mathcal{V} \setminus \mathcal{A})})$ at cost $\mathcal{O}(r^3)$. In typical RIG settings $s \ll r < m$, so repeated evaluation of these log-determinants quickly becomes the computational bottleneck. We refer to Equation (8) as the *Standard-MI* formulation.

B. Precomputation and an Alternate MI-RIG Objective

In MI-based RIG, the objective is evaluated repeatedly for many candidate sensing sets \mathcal{A} . This motivates *amortizing* computations that do not depend on \mathcal{A} . In particular, in Standard-MI (Equation (8)) the term $\det(\mathbf{K}_{\mathcal{V}\mathcal{V}})$ depends only on the fixed candidate set \mathcal{V} and can therefore be computed once and reused. With this precomputation, the per-evaluation cost drops from $\mathcal{O}(m^3)$ to $\mathcal{O}(r^3)$, and the dominant remaining computation becomes $\det(\mathbf{K}_{(\mathcal{V} \setminus \mathcal{A})(\mathcal{V} \setminus \mathcal{A})})$.

However, under the standard RIG objective (Equation 5), the selected set \mathcal{A} appears in both arguments of the MI term, so $\mathcal{V} \setminus \mathcal{A}$ changes across evaluations and the expensive determinant above cannot be reused. To expose additional reusable structure, we instead consider the alternate objective

$$\mathcal{A}^* = \arg \max_{\mathcal{A} \subset \mathcal{V}} \mathbb{I}(\mathcal{A}; \mathcal{V}), \tag{9}$$

for which MI can be written as

$$\begin{aligned}
\mathbb{I}(\mathcal{A}; \mathcal{V}) &= H(\mathcal{A}) + H(\mathcal{V}) - H(\mathcal{V} \cup \mathcal{A}) \\
&= \frac{1}{2} \ln \left[\frac{\det(\mathbf{K}_{\mathcal{A}\mathcal{A}}) \cdot \det(\mathbf{K}_{\mathcal{V}\mathcal{V}})}{\det(\mathbf{K}_{(\mathcal{A} \cup \mathcal{V})(\mathcal{A} \cup \mathcal{V})})} \right].
\end{aligned} \tag{10}$$

This removes the problematic term $\det(\mathbf{K}_{(\mathcal{V} \setminus \mathcal{A})(\mathcal{V} \setminus \mathcal{A})})$, but introduces the determinant over the union set $\det(\mathbf{K}_{(\mathcal{A} \cup \mathcal{V})(\mathcal{A} \cup \mathcal{V})})$. If $\mathcal{A} \subset \mathcal{V}$, then $\mathcal{A} \cup \mathcal{V} = \mathcal{V}$ and the expression collapses to

$$\begin{aligned}
\mathbb{I}(\mathcal{A}; \mathcal{V}) &= \frac{1}{2} \ln \left[\frac{\det(\mathbf{K}_{\mathcal{A}\mathcal{A}}) \cdot \det(\mathbf{K}_{\mathcal{V}\mathcal{V}})}{\det(\mathbf{K}_{(\mathcal{A} \cup \mathcal{V})(\mathcal{A} \cup \mathcal{V})})} \right] \\
&= \frac{1}{2} \ln \left[\frac{\det(\mathbf{K}_{\mathcal{A}\mathcal{A}}) \cdot \det(\mathbf{K}_{\mathcal{V}\mathcal{V}})}{\det(\mathbf{K}_{\mathcal{V}\mathcal{V}})} \right] \\
&= \frac{1}{2} \ln [\det(\mathbf{K}_{\mathcal{A}\mathcal{A}})],
\end{aligned} \tag{11}$$

i.e., the objective degenerates to the entropy of the selected set \mathcal{A} .

While this loses the MI coupling between the selected set \mathcal{A} and the unsampled locations $\mathcal{V} \setminus \mathcal{A}$, the next subsection shows how to recover the exact MI using a nondegenerate surrogate construction together with a Schur-complement factorization, enabling further computational savings.

C. Nondegenerate Schur-Complement-Based MI: Schur-MI

We now resolve the degeneracy that occurs when $\mathcal{A} \subset \mathcal{V}$. Our key idea is to break the exact set inclusion by introducing a *noisy surrogate* of the candidate set:

$$\mathcal{G} \triangleq \mathcal{V} + \epsilon, \quad \epsilon \sim \mathcal{N}(\mathbf{0}, \sigma^2 \mathbf{I}),$$

with σ chosen as a small fraction of the unit distance so that \mathcal{G} remains a near-copy of \mathcal{V} but does not coincide with it exactly. We then solve

$$\mathcal{A}^* = \arg \max_{\mathcal{A} \subset \mathcal{G}} \mathbb{I}(\mathcal{A}; \mathcal{V}). \tag{12}$$

Unlike the degenerate case, this objective does not collapse to the entropy of \mathcal{A} ; it preserves the full MI coupling between the selected set \mathcal{A} and the candidate set \mathcal{V} .

However, naively evaluating $\mathbb{I}(\mathcal{A}; \mathcal{V})$ from Equation (10) would require determinants over the union set $\mathcal{A} \cup \mathcal{V}$, with complexity $\mathcal{O}((s + m)^3)$ when $\mathcal{A} \not\subset \mathcal{V}$, which is worse than Standard-MI in Equation (8). We avoid this cost by leveraging the *Schur-complement*. The joint covariance over $\mathcal{A} \cup \mathcal{V}$ has the block form

$$\det(\mathbf{K}_{(\mathcal{A} \cup \mathcal{V})(\mathcal{A} \cup \mathcal{V})}) = \begin{bmatrix} \mathbf{K}_{\mathcal{A}\mathcal{A}} & \mathbf{K}_{\mathcal{A}\mathcal{V}} \\ \mathbf{K}_{\mathcal{V}\mathcal{A}} & \mathbf{K}_{\mathcal{V}\mathcal{V}} \end{bmatrix}, \tag{13}$$

the determinant of this block matrix can be expressed via the Schur-complement [20] as:

$$\begin{aligned}
\det(\mathbf{K}_{(\mathcal{A} \cup \mathcal{V})(\mathcal{A} \cup \mathcal{V})}) &= \det(\mathbf{K}_{\mathcal{V}\mathcal{V}}) \\
&\quad \cdot \det(\mathbf{K}_{\mathcal{A}\mathcal{A}} - \mathbf{K}_{\mathcal{A}\mathcal{V}} \mathbf{K}_{\mathcal{V}\mathcal{V}}^{-1} \mathbf{K}_{\mathcal{V}\mathcal{A}}) \\
&= \det(\mathbf{K}_{\mathcal{V}\mathcal{V}}) \cdot \det(\mathbf{K}_{\mathcal{A}|\mathcal{V}}),
\end{aligned} \tag{14}$$

where $\mathbf{K}_{\mathcal{A}|\mathcal{V}}$ is the conditional covariance of \mathcal{A} given \mathcal{V} . Substituting Equation (14) into Equation (10) yields the *Schur-MI* objective:

$$\begin{aligned}
\mathbb{I}(\mathcal{A}; \mathcal{V}) &= \frac{1}{2} \ln \left[\frac{\det(\mathbf{K}_{\mathcal{A}\mathcal{A}}) \cdot \det(\mathbf{K}_{\mathcal{V}\mathcal{V}})}{\det(\mathbf{K}_{(\mathcal{A} \cup \mathcal{V})(\mathcal{A} \cup \mathcal{V})})} \right] \\
&= \frac{1}{2} \ln \left[\frac{\det(\mathbf{K}_{\mathcal{A}\mathcal{A}}) \cdot \det(\mathbf{K}_{\mathcal{V}\mathcal{V}})}{\det(\mathbf{K}_{\mathcal{V}\mathcal{V}}) \cdot \det(\mathbf{K}_{\mathcal{A}|\mathcal{V}})} \right] \\
&= \frac{1}{2} \ln \left[\frac{\det(\mathbf{K}_{\mathcal{A}\mathcal{A}})}{\det(\mathbf{K}_{\mathcal{A}|\mathcal{V}})} \right] \\
&= \frac{1}{2} \ln \left[\frac{\det(\mathbf{K}_{\mathcal{A}\mathcal{A}})}{\det(\mathbf{K}_{\mathcal{A}\mathcal{A}} - \mathbf{K}_{\mathcal{A}\mathcal{V}} \mathbf{K}_{\mathcal{V}\mathcal{V}}^{-1} \mathbf{K}_{\mathcal{V}\mathcal{A}})} \right].
\end{aligned} \tag{15}$$

Schur-MI is mathematically equivalent to Standard-MI (Equation (8)), but exposes substantial structure for efficient evaluation. In particular, $\mathbf{K}_{\mathcal{V}\mathcal{V}}^{-1}$ can be computed

once and reused across all candidate sets. With this pre-computation, evaluating Equation (15) requires only forming $\mathbf{K}_{\mathcal{A}\mathcal{V}}$ and computing determinants of $s \times s$ matrices, resulting in an effective cost of $\mathcal{O}(s^3)$ per MI evaluation.

Crucially, this formulation preserves the informativeness of the original MI-RIG objective $\mathbb{I}(\mathcal{A}; \mathcal{V} \setminus \mathcal{A})$: it captures information about the full environment while avoiding the degeneracy that arises when $\mathcal{A} \subset \mathcal{V}$. Empirically, our experiments (Section VI-B) show that, under greedy selection with a stationary GP kernel, the proposed RIG objective—combined with the noisy-surrogate candidate-set construction, Schur-MI, and precomputation—achieves the same Standard-MI value for the selected sensing locations as the original RIG formulation using Standard-MI (Eq. 5).

D. Reference Algorithm: Greedy Maximization of Schur-MI

Algorithm 1 summarizes the greedy approach for maximizing the proposed MI objective. Greedy MI maximization admits a *near-optimal approximation guarantee* due to submodularity [3].

We present greedy selection as a reference rather than a requirement: the proposed MI-RIG formulation can be optimized with a range of alternatives, including Bayesian optimization [5] and genetic algorithms [4]. Moreover, it readily accommodates practical constraints such as distance budgets and motion feasibility, consistent with prior work [12], [7].

Algorithm 1: Greedy sensor placement via Schur-MI with precomputation.

Input: Candidate locations \mathcal{V} , number of sensing locations s , kernel $k(\cdot, \cdot)$, noise σ^2 .
Output: Solution locations \mathcal{A}^* .
 // Noisy surrogate set
 1 Sample $\epsilon \sim \mathcal{N}(\mathbf{0}, \sigma^2 \mathbf{I})$ and set $\mathcal{G} \leftarrow \mathcal{V} + \epsilon$
 // Precompute inverse
 2 $\mathbf{K}_{\mathcal{V}\mathcal{V}} \leftarrow k(\mathcal{V}, \mathcal{V})$; $\mathbf{K}_{\text{const}} \leftarrow \mathbf{K}_{\mathcal{V}\mathcal{V}}^{-1}$
 // Initialize
 3 $\mathcal{A}^* \leftarrow \emptyset$; $\delta_{\text{base}} \leftarrow 0$
 4 **for** $j \leftarrow 1$ **to** s **do** // Greedy selection
 5 **foreach** $a \in \mathcal{G}$ **do** // Marginal gain
 6 $\mathcal{A} \leftarrow \mathcal{A}^* \cup \{a\}$
 7 $\delta(a) \leftarrow \frac{1}{2} \ln \left[\frac{\det(\mathbf{K}_{\mathcal{A}\mathcal{A}})}{\det(\mathbf{K}_{\mathcal{A}\mathcal{A}} - \mathbf{K}_{\mathcal{A}\mathcal{V}} \mathbf{K}_{\text{const}} \mathbf{K}_{\mathcal{A}\mathcal{V}}^\top)} \right] - \delta_{\text{base}}$
 // Select and update solution set
 8 $a^* \leftarrow \arg \max_{a \in \mathcal{G}} \delta(a)$
 9 $\mathcal{A}^* \leftarrow \mathcal{A}^* \cup \{a^*\}$
 // Update baseline
 10 $\delta_{\text{base}} \leftarrow \frac{1}{2} \ln \left[\frac{\det(\mathbf{K}_{\mathcal{A}^*\mathcal{A}^*})}{\det(\mathbf{K}_{\mathcal{A}^*\mathcal{A}^*} - \mathbf{K}_{\mathcal{A}^*\mathcal{V}} \mathbf{K}_{\text{const}} \mathbf{K}_{\mathcal{A}^*\mathcal{V}}^\top)} \right]$
 11 **return** \mathcal{A}^*

VI. EXPERIMENTS

This section details the experiments used to evaluate the effectiveness and computational efficiency of Schur-MI.

A. MI-Based Methods in Discrete Environments

We first benchmark Standard-MI against discrete-space optimal design metrics—A-, B-, and D-optimality [7]—to verify MI’s empirical advantages in sensor placement. All metrics were optimized using greedy selection. For MI, we additionally evaluated the lazy greedy algorithm [3], which retains the approximation guarantees of standard greedy while reducing the number of objective evaluations via a priority-queue strategy.

We evaluated sensor placement (SP) on four bathymetry datasets—Mississippi, Nantucket, Virgin Islands, and Wrangell [21]. We used a Gaussian process (GP) with a radial basis function (RBF) kernel [1], trained on 1000 randomly sampled points from each environment, and a randomly sampled set of 500 candidate sensing locations \mathcal{V} . Performance was evaluated for sensing set sizes from 5 to 100 in increments of 5, with 10 trials per setting.

Fig 2 (standardized mean squared error; SMSE [1]) and Fig 3 (runtime) summarize the results. Consistent with prior work [3], MI outperform the optimal-design baselines in reconstruction accuracy (SMSE). Greedy and lazy greedy achieve identical SMSE, but lazy greedy is substantially faster due to fewer MI evaluations. A-optimality attains unexpectedly strong SMSE on Nantucket, which we attribute to a mismatch between the stationary RBF kernel and the dataset’s non-stationary spatial structure. Overall, these results confirm that the Standard-MI objective optimized with lazy greedy remains a strong and reliable baseline for discrete-space sensor placement.

B. Schur-MI with Precomputation

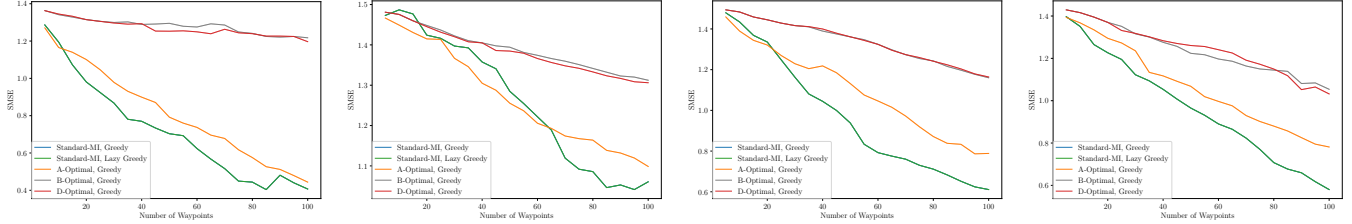
Next, we compare Schur-MI to Standard-MI, each evaluated with and without precomputation (PC). All methods were optimized using lazy greedy. Fig 4 and Fig 5 report runtime and Standard-MI values across the four datasets. As expected, all methods produce identical MI scores, confirming the equivalence of the four formulations.

Without PC, Schur-MI is slightly slower than Standard-MI, likely due to constant-factor overhead from additional matrix multiplications in the Schur formulation. With PC enabled, Schur-MI becomes the fastest approach, demonstrating the practical benefits of exposing reusable, invariant terms. Notably, Schur-MI with PC is faster than Standard-MI with PC. These results highlight the importance of the $\mathbb{I}(\mathcal{A}; \mathcal{V})$ formulation, which enables efficient reuse of precomputed matrix factors across MI evaluations.

C. Continuous-Space Evaluation

We next evaluate SP in a continuous-space setting. Baselines include A-, B-, and D-optimality, each optimized via gradient descent. We compare against Schur-MI with PC optimized using (i) lazy greedy, (ii) gradient descent, and (iii) CMA-ES (a derivative-free evolutionary optimizer [4]). We also include Continuous-SGP [22], which leverages sparse GP approximations for scalability.

Fig 6 and Fig 7 report SMSE and runtime, respectively. In reconstruction accuracy, Schur-MI (optimized via lazy



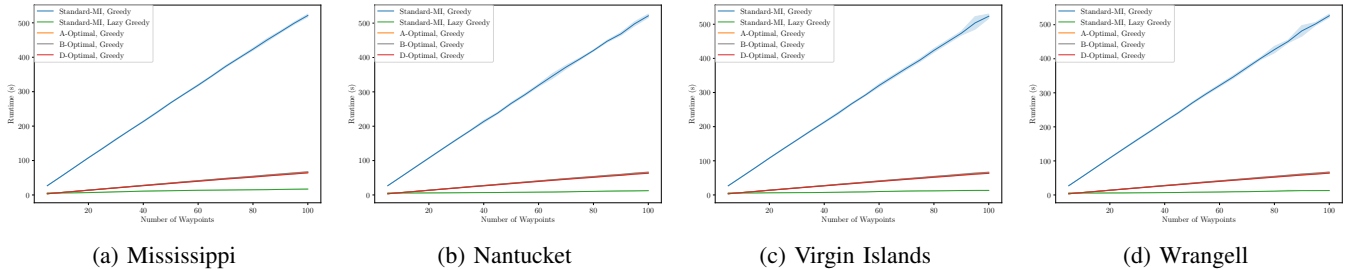
(a) Mississippi

(b) Nantucket

(c) Virgin Islands

(d) Wrangell

Fig. 2: SMSE for sensor placement, comparing MI with Bayesian optimal design objectives. Curves show mean \pm standard deviation of SMSE versus the number of waypoints; lower is better. Because the greedy methods are deterministic, results variability was negligible. These results highlight the performance advantage of MI-based objectives for discrete-space SP.



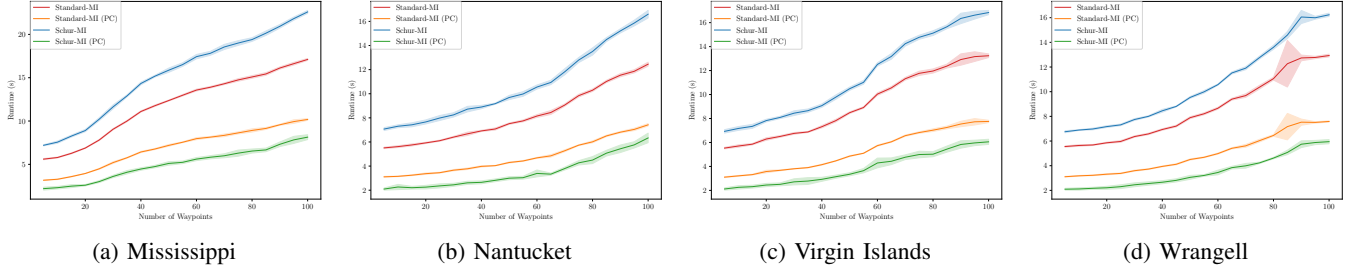
(a) Mississippi

(b) Nantucket

(c) Virgin Islands

(d) Wrangell

Fig. 3: Runtime for sensor placement, comparing MI with Bayesian optimal design objectives. Curves show mean \pm standard deviation of Runtime versus the number of waypoints; lower is better.



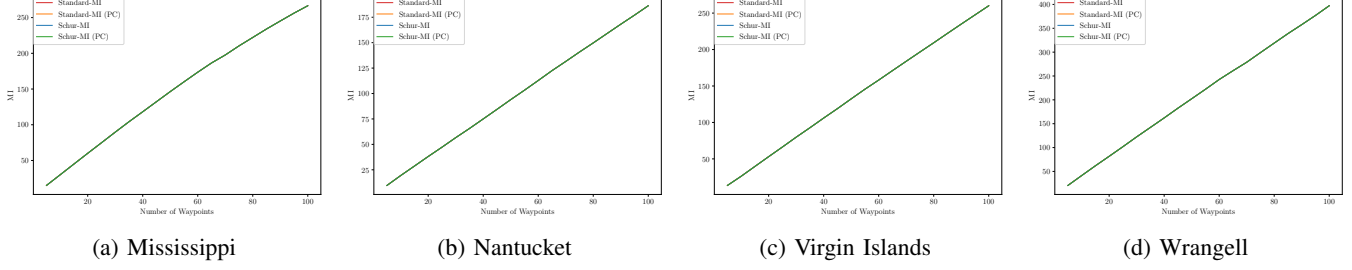
(a) Mississippi

(b) Nantucket

(c) Virgin Islands

(d) Wrangell

Fig. 4: Runtime for SP across MI formulations. Curves show mean \pm standard deviation of runtime versus the number of waypoints; lower is better. Schur-MI with PC is consistently the fastest MI formulation.



(a) Mississippi

(b) Nantucket

(c) Virgin Islands

(d) Wrangell

Fig. 5: Runtime for SP across MI formulations. Curves show mean \pm standard deviation of runtime versus the number of waypoints; lower is better. The results show that all four MI formulations are equivalent.

greedy and CMA-ES), A-optimality, and Continuous-SGP perform similarly, achieving low SMSE across datasets. In contrast, Schur-MI optimized via gradient descent underperforms, likely due to sensitivity to local minima despite the objective being fully differentiable.

In runtime, A-optimality and Continuous-SGP are consistently the most efficient. Overall, these results suggest

that for continuous-space sensor placement, A-optimality and Continuous-SGP currently provide the best accuracy–runtime trade-off, while Schur-MI remains competitive, particularly when optimized with CMA-ES.

For discrete-space sensor placement, Schur-MI combined with PC yields the best overall performance, improving runtime relative to Standard-MI while preserving the sub-

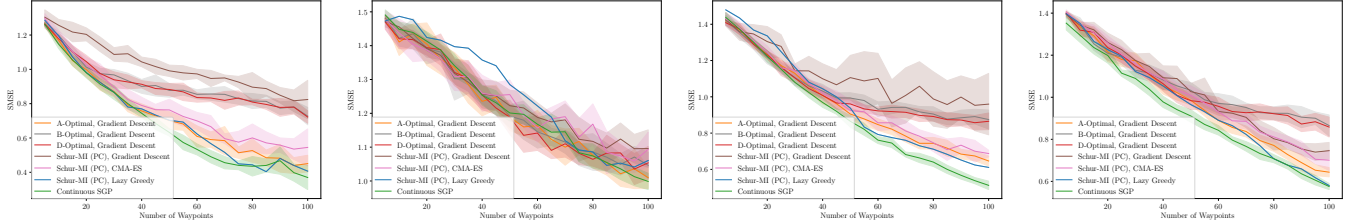


Fig. 6: SMSE for SP in continuous space. Curves show mean \pm standard deviation of SMSE versus the number of waypoints; lower is better. MI-based objectives remain competitive in continuous spaces.

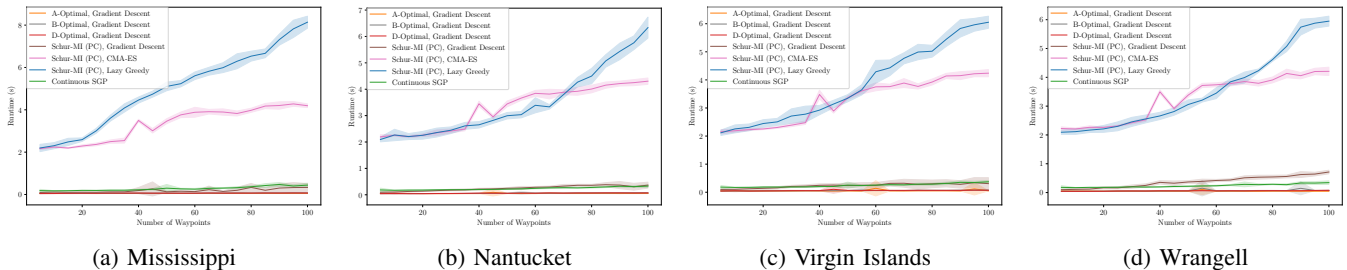


Fig. 7: Runtime for SP in continuous space. Curves show mean \pm standard deviation of Runtime versus the number of waypoints; lower is better. MI-based objectives remain competitive in continuous spaces.

modular approximation guarantee. Together, these findings support Schur-MI as a principled and efficient objective for robotic information gathering.

D. Schur-MI with Non-Stationary Kernels

We further compare Schur-MI with PC to Standard-MI in a SP task using a GP with a non-stationary kernel [18]. Unlike the stationary RBF kernel, the attentive kernel can capture spatially varying covariance structure. We use the Nantucket bathymetry dataset [21] and randomly sample 300 candidate sensing locations \mathcal{V} . SP was performed with lazy greedy [3]. Fig 8 reports mean and standard deviation of SMSE, along with runtime.

Schur-MI consistently achieves lower SMSE than Standard-MI, with the gap increasing for larger sensing sets. We attribute this to the $\mathcal{V} \setminus \mathcal{A}$ term in Standard-MI, which can induce spatial bias toward unsensed regions rather than reflecting information gain with respect to the

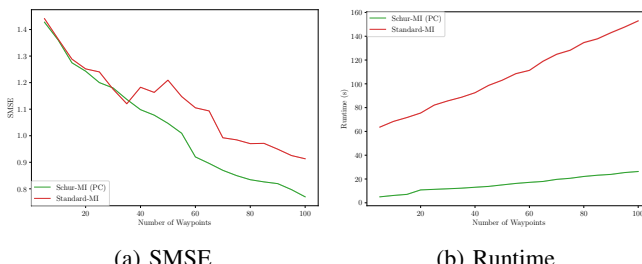


Fig. 8: SMSE (left) and runtime (right) for SP with a non-stationary kernel. Curves show mean \pm standard deviation versus the number of waypoints; lower is better. Schur-MI achieves substantial gains with non-stationary kernels.

environment as a whole. Additionally, Schur-MI with PC yields up to a $12.7 \times$ speedup over the standard formulation. These results emphasize both the accuracy and computational advantages of Schur-MI with PC, particularly under non-stationary modeling.

E. Field Trial Deployment

To assess real-world applicability, we deployed our method on an autonomous surface vehicle (ASV) [23] in a lake. The ASV (Fig 1) was equipped with GPS, a single-beam sonar, and a Raspberry Pi 5 for onboard computation.

We conducted an informative path planning (IPP) trial in which the planner iteratively updated an online GP model by updating hyperparameters from collected data and replanning the remaining waypoints to maximize information gain. Following the IPP framework of Jakkala and Akella [8], we used Schur-MI with PC as the objective, an RBF kernel for the GP model, and optimized 20 waypoints using CMA-ES.

To evaluate reconstruction quality, we performed a dense boustrophedon survey of the environment to serve as ground truth. The IPP-generated data was then used to reconstruct the bathymetry and the posterior variance (Fig 9). The reconstruction achieved an SMSE of 4.54 and an RMSE of 0.60. The disparity between these metrics is attributed to elevated predictive uncertainty in unvisited regions—an expected outcome given the RBF kernel's finite length scale.

Overall, the ASV successfully executed an adaptive, data-driven path under real-time sensing and compute constraints. These results demonstrate that Schur-MI is theoretically well-grounded and also practical for field-deployable RIG.

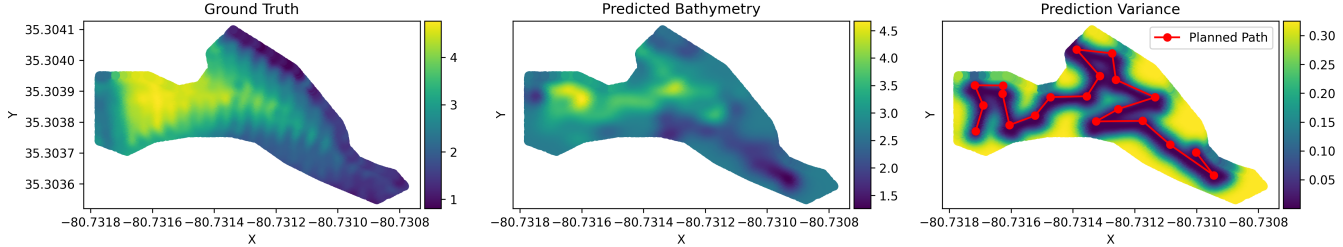


Fig. 9: Field trial results: ground truth (left), reconstruction along the planned path (middle), and predictive variance (right). All color bars are in meters. These results demonstrate that Schur-MI is theoretically well-grounded and practical for field-deployable RIG.

VII. CONCLUSION

We presented **Schur-MI**, a computationally efficient mutual information (MI) objective for Gaussian process (GP)-based robotic information gathering (RIG). Schur-MI combines a Schur-complement factorization of the MI criterion with a precomputation strategy that leverages the iterative structure of RIG planners. Together, these techniques reduce the per-evaluation cost of MI from $\mathcal{O}(|\mathcal{V}|^3)$ to $\mathcal{O}(|\mathcal{A}|^3)$, where \mathcal{V} and \mathcal{A} denote the candidate and selected sensing sets.

Across both discrete and continuous domains, our experiments show that Schur-MI retains the informativeness of Standard-MI while substantially reducing runtime. In continuous spaces, it is competitive with established baselines such as A-optimal design and Continuous-SGP. In discrete settings, it consistently improves on Standard-MI in runtime and achieves comparable or better reconstruction accuracy, while preserving the near-optimal approximation guarantee of greedy MI-based selection.

Field trials on a compute-limited autonomous surface vehicle (ASV) further demonstrate that Schur-MI enables adaptive informative path planning (IPP) under real-world constraints.

Overall, by making MI evaluation tractable for iterative, online planning, **Schur-MI helps bridge the gap between information-theoretic objectives and real-time robotic exploration**, enabling resource-aware autonomy in complex and uncertain environments.

REFERENCES

- [1] C. E. Rasmussen and C. K. I. Williams, *Gaussian Processes for Machine Learning*. Cambridge, USA: MIT Press, 2005.
- [2] W. Caselton and J. Zidek, “Optimal monitoring network designs,” *Statistics & Probability Letters*, vol. 2, no. 4, pp. 223–227, 1984.
- [3] A. Krause, A. Singh, and C. Guestrin, “Near-Optimal Sensor Placements in Gaussian Processes: Theory, Efficient Algorithms and Empirical Studies,” *Journal of Machine Learning Research*, vol. 9, no. 8, pp. 235–284, 2008.
- [4] G. Hitz, E. Galceran, M.-E. Garneau, F. Pomerleau, and R. Siegwart, “Adaptive Continuous-Space Informative Path Planning for Online Environmental Monitoring,” *Journal of Field Robotics*, vol. 34, no. 8, pp. 1427–1449, 2017.
- [5] G. Francis, L. Ott, R. Marchant, and F. Ramos, “Occupancy map building through Bayesian exploration,” *The International Journal of Robotics Research*, vol. 38, no. 7, pp. 769–792, 2019.
- [6] X. Lin, A. Chowdhury, X. Wang, and G. Terejanu, “Approximate computational approaches for Bayesian sensor placement in high dimensions,” *Information Fusion*, vol. 46, pp. 193–205, 2019.
- [7] J. Ott, M. J. Kochenderfer, and S. Boyd, “Approximate sequential optimization for informative path planning,” *Robotics and Autonomous Systems*, vol. 182, p. 104814, 2024.
- [8] K. Jakkala and S. Akella, “Fully Differentiable Adaptive Informative Path Planning,” in *2025 IEEE International Conference on Robotics and Automation*, Atlanta, GA, May 2025, pp. 5431–5437.
- [9] D. Ramsden, “Optimization approaches to sensor placement problems,” Ph.D. dissertation, Department of Mathematical Sciences, Rensselaer Polytechnic Institute, August 2009.
- [10] M. Schwager, M. P. Vitus, S. Powers, D. Rus, and C. J. Tomlin, “Robust adaptive coverage control for robotic sensor networks,” *IEEE Transactions on Control of Network Systems*, vol. 4, no. 3, 2017.
- [11] J. Binney, A. Krause, and G. S. Sukhatme, “Optimizing waypoints for monitoring spatiotemporal phenomena,” *The International Journal of Robotics Research*, vol. 32, no. 8, pp. 873–888, 2013.
- [12] J. Ott, E. Balaban, and M. J. Kochenderfer, “Sequential Bayesian optimization for adaptive informative path planning with multimodal sensing,” in *International Conference on Robotics and Automation (ICRA)*, 2023.
- [13] S. Manjanna and G. Dudek, “Data-driven selective sampling for marine vehicles using multi-scale paths,” in *2017 IEEE/RSJ International Conference on Intelligent Robots and Systems (IROS)*, 2017.
- [14] J. Rückin, L. Jin, and M. Popović, “Adaptive Informative Path Planning Using Deep Reinforcement Learning for UAV-based Active Sensing,” in *2022 International Conference on Robotics and Automation (ICRA)*, 2022, pp. 4473–4479.
- [15] A. Asgharivaskasi, S. Koga, and N. Atanasov, “Active Mapping via Gradient Ascent Optimization of Shannon Mutual Information over Continuous SE(3) Trajectories,” in *2022 IEEE/RSJ International Conference on Intelligent Robots and Systems (IROS)*, 2022.
- [16] K. Jakkala and S. Akella, “Fully differentiable sensor placement and informative path planning,” *The International Journal of Robotics Research*, 2025.
- [17] G. Tajnafoi, R. Arcucci, L. Mottet, C. Vouriot, M. Molina-Solana, C. Pain, and Y.-K. Guo, “Variational Gaussian Process for Optimal Sensor Placement,” *Applications of Mathematics*, vol. 66, no. 2, pp. 287–317, Apr 2021.
- [18] W. Chen, R. Khordon, and L. Liu, “AK: Attentive Kernel for Information Gathering,” in *Proceedings of Robotics: Science and Systems*, New York City, NY, USA, June 2022.
- [19] W. Chen, L. Liu, and R. Khordon, “POAM: Probabilistic Online Attentive Mapping for Efficient Robotic Information Gathering,” in *Robotics: Science and Systems*, 2024.
- [20] C. Bishop, *Pattern Recognition and Machine Learning*, ser. Information Science and Statistics. Springer New York, 2006.
- [21] NOAA. Digital Coast: NOAA Office for Coastal Management. [Online]. Available: <https://coast.noaa.gov/digitalcoast/>
- [22] K. Jakkala and S. Akella, “Multi-Robot Informative Path Planning from Regression with Sparse Gaussian Processes,” in *2024 IEEE International Conference on Robotics and Automation (ICRA)*, 2024.
- [23] M. Brancato and A. Wolek, “Adaptive Sampling of a Stationary Gaussian Spatial Process by a Team of Robots With Heterogeneous Dynamics and Measurement Noise Variance,” *IEEE Access*, vol. 12, pp. 94 407–94 423, 2024.